JOURNAL OF THERMOPHYSICS AND HEAT TRANSFER
Vol. 23, No. 1, January–March 2009

Non-Newtonian Natural Convection Along a Vertical Plate with Uniform Surface Heat Fluxes

M. M. Molla*
University of Glasgow, Glasgow, Scotland G12 8QQ, United Kingdom
and
L. S. Yao†
Arizona State University, Tempe, Arizona 85287

DOI: 10.2514/1.37566

Natural convection of non-Newtonian fluids along a vertical flat plate with the heating condition of uniform surface heat flux was investigated using a modified power-law viscosity model. In this model, there are no physically unrealistic limits in the boundary-layer formulation for power-law non-Newtonian fluids. The governing equations are transformed into parabolic coordinates and the singularity of the leading edge is removed; hence, the boundary-layer equations can be solved straightforwardly by marching from the leading edge downstream. Numerical results are presented for the case of shear-thinning as well as shear-thickening fluids for two limits. The numerical results demonstrate that a similarity solution for natural convection exists near the leading edge, where the shear rate is not large enough to trigger non-Newtonian effects. After the shear rate increases beyond a threshold value, non-Newtonian effects start to develop and a similarity solution no longer exists. This indicates that the length scale is introduced into the boundary-layer formulation by the classical power-law correlation.

Nomenclature

C	=	constant
C_f	=	dimensionless skin-friction coefficient
D	=	nondimensional viscosity of the fluid
Gr	=	Grashof number
K	=	constant, thermal conductivity
L	=	reference length scale of the plate
N	=	non-Newtonian power-law index
q_w	=	surface heat flux
T	=	dimensional temperature of the fluid
T_∞	=	ambient temperature
U, V	=	dimensionless fluid velocity components in the ξ, ηdirections
$\bar{u}, \bar{v}$	=	fluid velocity components in the $\bar{x}$, $\bar{y}$directions
α	=	thermal diffusivity
γ	=	shear rate
η	=	pseudosimilarity variable
θ	=	dimensionless temperature of the fluid
θ_w	=	surface temperature
ν	=	viscosity of the non-Newtonian fluid
ν_1	=	reference viscosity of the fluid
ξ	=	axial direction along the plate
ρ	=	fluid density

I. Introduction

THE major motivation for studying the dynamics of non-Newtonian power-law fluids is their importance in many practical applications. The interest in heat transfer problems involving power-law non-Newtonian fluids has grown in the past half-century. A sequence of excellent lectures on non-Newtonian fluids was given by Hinch [1]. It appears that Acrivos [2], in a frequently cited paper, was the first to consider boundary-layer flows for such fluids. Since then, a large number of papers have been published, due to their wide relevance in chemicals, foods, polymers, molten plastics and petroleum production, and various natural phenomena. A complete survey of this literature is impractical; however, selected papers are listed here to provide starting points for a broader literature search [3–15].

Two common mistakes often appear in papers that study boundary layers of power-law non-Newtonian fluids. The first is that few authors recognize that their approach introduces a length scale into their formulations; consequently, boundary-layer problems with power-law non-Newtonian fluids cannot have self-similar solutions. Nevertheless, it is convenient practice to ignore the dependence on the streamwise coordinate. It has been demonstrated in [16] that such a self-similar solution is actually only valid at the leading edge of the boundary layer. The similarity solution is a natural upstream condition, which is needed to integrate boundary-layer equations along the streamwise direction from the leading edge.

The second concern is related to the unrealistic physical result, introduced by the traditional power-law correlation, that viscosity either vanishes or becomes infinite in the limits of large or small shear rates, respectively. This usually occurs at the leading edge of a flat plate or along the outer edge of boundary layers, where the boundary layer matches the outer inviscid flow. Thus, power-law correlations introduce nonremovable singularities into boundary-layer formulations for an infinite or zero viscosity. Without recognizing the cause of such unrealistic conditions, a false-starting process has been used to integrate boundary-layer equations slightly downstream from the leading edge to avoid the leading-edge region; sometimes, complex multilayer structures have been introduced to overcome mathematical difficulties to obtain solutions of a nonphysical formulation [14,15].

The recently proposed modified power-law correlation is sketched for various power indices n in Fig. 1 and this model is formulated based on the available experimental data for the non-Newtonian fluids (see Hinch [1]). It is clear that the new correlation does not contain the physically unrealistic limits of zero and infinite viscosity displayed by traditional power-law correlations [2]. The modified power law, in fact, fits data well. The constants in the proposed model can be fixed with available measurements and are described in detail in [16]. The boundary-layer formulation on a flat plate is described and numerically solved in [16], and the associated heat transfer for two different heating conditions is reported in [17] for a shear-thinning fluid. In this investigation, the behaviors of both

Received 15 March 2008; revision received 22 July 2008; accepted for publication 25 July 2008.

*Department of Mechanical Engineering.
†Department of Mechanical and Aerospace Engineering.

shear-thinning and shear-thickening fluids on the natural-convection laminar flow with uniform heat-flux heating condition are studied by choosing the power-law index as $n = 0.6, 0.8, 1, 1.2$, and 1.4 to fully demonstrate the performance of various non-Newtonian fluids.

It is worthy to note that the validity of the laminar boundary-layer theory has been well established for nearly a century. Power-law correlations have also been used for nearly half a century. It is well known that they can correlate a major part of the available data. The recently proposed modified power law simply modifies the power law to fit available data better at its two ends, because a power-law model is a direct model that is used to fit experimental data. The results of our parametric study in the paper can provide the necessary database that a simple interpolation can be used to find approximate heat transfer rates and wall shear stresses for any non-Newtonian fluid from our tables.

Our study also indicates the importance of measuring a complete set of viscosity-shear relations. Because an infinite viscosity corresponds to solids and no frictionless fluid has ever been found, a partial set of measured viscosity-shear relations is not sufficient for a boundary-layer study.

II. Formulation of the Problem

A steady laminar boundary layer of a non-Newtonian fluid on a semi-infinite flat plate with uniform heat flux was studied. The viscosity depends on shear rate and is correlated by a modified power law. We consider shear-thinning and shear-thickening situations of non-Newtonian fluids. It is assumed that a surface heat flux q_w is applied to the plate; T_∞ is the ambient temperature of the fluid. The coordinate system is shown in Fig. 2, in which δ_M and δ_T represent the momentum and thermal boundary-layer thickness, respectively.

The boundary-layer equations for the flow and heat transfer are

$$\frac{\partial \bar{u}}{\partial \bar{x}} + \frac{\partial \bar{v}}{\partial \bar{y}} = 0 \tag{1}$$

$$\bar{u}\frac{\partial \bar{u}}{\partial \bar{x}} + \bar{v}\frac{\partial \bar{u}}{\partial \bar{y}} = \frac{\partial}{\partial \bar{y}}\left(\nu \frac{\partial \bar{u}}{\partial \bar{y}}\right) + g\beta(T - T_\infty) \tag{2}$$

$$\bar{u}\frac{\partial T}{\partial \bar{x}} + \bar{v}\frac{\partial T}{\partial \bar{y}} = \alpha \frac{\partial^2 T}{\partial \bar{y}^2} \tag{3}$$

where $\bar{u}$ and $\bar{v}$ are velocity components along the $\bar{x}$ and $\bar{y}$ axes, T is the temperature of the fluid, g is the acceleration due to gravity, β is the thermal expansion coefficient, and α is the thermal diffusivity of the fluid. The viscosity is correlated by a modified power law, which is

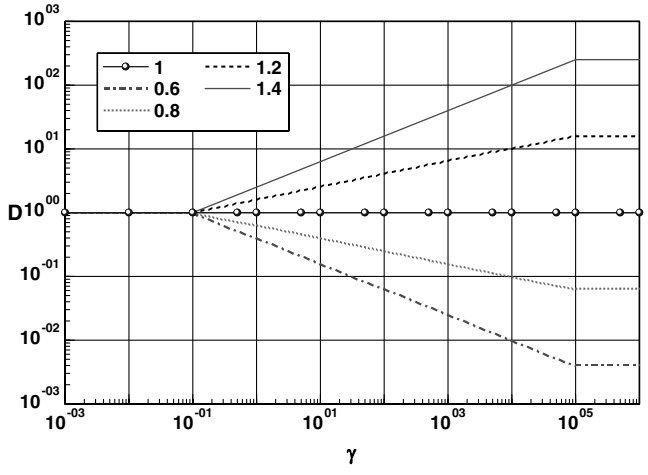

Fig. 1 Modified power-law correlation for the first set of shears.

$$\nu = \frac{K}{\rho}\left|\frac{\partial \bar{u}}{\partial \bar{y}}\right| \quad \text{for } \bar{\gamma}_1 \le \left|\frac{\partial \bar{u}}{\partial \bar{y}}\right| \le \bar{\gamma}_2 \tag{4}$$

The constants $\bar{\gamma}_1$ and $\bar{\gamma}_2$ are threshold shear rates, which are given according to the experimental data of Hinch [1], ρ is the density of the fluid, and K is a dimensional constant, for which the dimension depends on the power-law index n. The values of these constants can be determined by matching with measurements. Outside of the preceding range, viscosity is assumed to be constant; its value can be fixed with data given in Fig. 1.

The boundary conditions for the present problem are

$$\bar{u} = \bar{v} = 0, \qquad -k\frac{\partial T}{\partial \bar{y}} = q_w \quad \text{at } \bar{y} = 0 \tag{5a}$$

$$\bar{u} \to 0, \qquad T \to T_\infty \quad \text{as } \bar{y} \to \infty \tag{5b}$$

The required upstream conditions will be provided later. We now introduce the following nondimensional transformations:

$$x = \frac{\bar{x}}{l}, \qquad y = \frac{\bar{y}}{l}Gr^{1/5}, \qquad u = \frac{l}{\nu_1}Gr^{-2/5}\bar{u}$$
$$v = \frac{l}{\nu_1}Gr^{-1/5}\bar{v}, \qquad \Theta = \frac{T - T_\infty}{(q_w l/k)}Gr^{1/5}, \qquad Gr = \frac{g\beta q_w l^4}{k\nu_1^2} \tag{6}$$
$$Pr = \frac{\nu_1}{\alpha}, \qquad D = \frac{\nu}{\nu_1}$$

where ν_1 is the reference viscosity at $\bar{\gamma}_1$, Θ is the dimensionless temperature of the fluid, Gr is the Grashof number, and Pr is the Prandtl number. Using Eq. (6) in Eqs. (1–4), we get the following nondimensional equations:

$$\frac{\partial u}{\partial x} + \frac{\partial v}{\partial y} = 0 \tag{7}$$

$$u\frac{\partial u}{\partial x} + v\frac{\partial u}{\partial y} = \frac{\partial}{\partial y}\left(D\frac{\partial u}{\partial y}\right) + \Theta \tag{8}$$

$$u\frac{\partial \Theta}{\partial x} + v\frac{\partial \Theta}{\partial y} = \frac{1}{Pr}\frac{\partial^2 \Theta}{\partial y^2} \tag{9}$$

$$D = \frac{K}{\rho\nu_1}\left|\frac{\nu_1}{l^2}Gr^{3/5}\frac{\partial u}{\partial y}\right|^{n-1}$$
$$= \frac{K}{\rho\nu_1}\left(\frac{\nu_1}{l^2}\right)^{n-1}\left[\left(\frac{g\beta q_w l^4}{k\nu_1^2}\right)^{3/5}\right]^{n-1}\left|\frac{\partial u}{\partial y}\right|^{n-1} = C\left|\frac{\partial u}{\partial y}\right|^{n-1} \tag{10}$$

The length scale associated with the non-Newtonian power law is

$$l = C^{\frac{5}{2(n-1)}}\left[\left(\frac{K}{\rho}\right)^{5/2}\frac{1}{\nu_1^{n+4}}\right]^{\frac{1}{1-n}}\left[\frac{k}{g\beta q_w}\right]^{3/2} \tag{11}$$

Now we introduce the parabolic transformation as in [18]:

$$\xi = x, \qquad \eta = \frac{y}{(5x)^{1/5}}, \qquad U = \frac{u}{(5x)^{3/5}}$$
$$V = (5x)^{1/5}v, \qquad \theta = \frac{\Theta}{(5x)^{1/5}} \tag{12}$$

Substituting variables (12) into Eqs. (7–10) leads to the following equations:

$$(5\xi)\frac{\partial U}{\partial \xi} + 3U - \eta\frac{\partial U}{\partial \eta} + \frac{\partial V}{\partial \eta} = 0 \tag{13}$$

$$(5\xi)U\frac{\partial U}{\partial \xi}+(V-\eta U)\frac{\partial U}{\partial \eta}+3U^2=\frac{\partial}{\partial \eta}\left[D\frac{\partial U}{\partial \eta}\right]+\theta \tag{14}$$

$$(5\xi)U\frac{\partial \theta}{\partial \xi}+(V-\eta U)\frac{\partial \theta}{\partial \eta}+U\theta=\frac{1}{Pr}\frac{\partial^2\theta}{\partial \eta^2} \tag{15}$$

$$\gamma=(5\xi)^{5/2}\frac{\partial U}{\partial \eta} \tag{16}$$

$$D=\begin{cases}1, & |\gamma|\le\gamma_1\\ \left|\frac{\gamma}{\gamma_1}\right|^{n-1}, & \gamma_1\le|\gamma|\le\gamma_2\\ \left|\frac{\gamma_2}{\gamma_1}\right|^{n-1}, & |\gamma|\ge\gamma_2\end{cases} \tag{17}$$

Correlation (17) is similar to, but with different scales from, that proposed in [16], which is described for shear-thinning fluid oil at 68°F, for which the power-law index is $n=0.95$. The correlation for both the shear-thinning and shear-thickening fluids is presented in [19] for forced convections. The present correlation (17) is for natural convection and is the extended form of the model proposed in [16,19], which is for forced convection. The traditional power law is used to determine the viscosity when the shear rate falls in the range of $\gamma_1\le|\gamma|\le\gamma_2$; otherwise, viscosity either vanishes or becomes infinite at the limit of large or small shear rates, respectively. Also, the range of γ_1 and γ_2 is physically unrealistic. The present proposed correlation describes that if the shear rates $|\gamma_1|$ lie between the threshold shear rates γ_1 and γ_2, then the non-Newtonian viscosity D varies with the power law of γ. On the other hand, if the shear rates $|\gamma|$ do not lie within γ_1 and γ_2, then the non-Newtonian viscosities D are different constants, which are shown in Fig. 1. This is the property of many measured data of viscosities.

Equations (13–15) can be solved by marching downstream with the leading-edge condition satisfying the following differential equations, which are the limit of Eqs. (13–15) as $\xi\to 0$:

$$3U-\eta\frac{\partial U}{\partial \eta}+\frac{\partial V}{\partial \eta}=0 \tag{18}$$

$$(V-\eta U)\frac{\partial U}{\partial \eta}+3U^2=\frac{\partial}{\partial \eta}\left[D\frac{\partial U}{\partial \eta}\right]+\theta \tag{19}$$

$$(V-\eta U)\frac{\partial \theta}{\partial \eta}+U\theta=\frac{1}{Pr}\frac{\partial^2\theta}{\partial \eta^2} \tag{20}$$

The corresponding boundary conditions are

$$U=V=0,\qquad \frac{\partial\theta}{\partial\eta}=-1\quad \text{at } \eta=0 \tag{21a}$$

$$U\to 0,\qquad \theta\to 0\quad \text{as } \eta\to\infty \tag{21b}$$

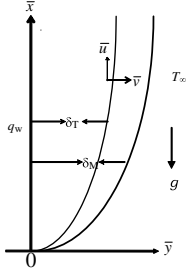

Fig. 2 Coordinates.

Equations (13–15) and (18–20) are discretized by a central-difference scheme for the diffusion term and a backward-difference scheme for the convection terms. Finally, we get a system of implicit tridiagonal algebraic system of equations, which can be solved by a double-sweep technique. The normal velocity is directly solved from the continuity equation. The computation is started at $\xi=0$, and the solution of Eqs. (13–15) is the upstream condition for marching downstream to $\xi=150$. After several test runs, converged results are obtained by using $\Delta\xi=0.01$ and $\Delta\eta=0.0025$.

In practical applications, the physical quantities of principle interest are the local skin-friction coefficient C_f and the local Nusselt number Nu, which are

$$C_f\left[\frac{Gr}{(5\xi)^2}\right]^{1/5}=\left[D\frac{\partial U}{\partial \eta}\right]_{\eta=0} \tag{22}$$

$$Nu\left(\frac{Gr}{5\xi}\right)^{-1/5}=\frac{1}{\theta(\xi,0)} \tag{23}$$

The average Nusselt number is obtained based on the average plate minus temperature. Thus,

$$Nu_m=\frac{q_w l}{k(T_w-T_\infty)_m} \tag{24}$$

where

$$(T_w-T_\infty)_m=\frac{1}{s}\int_0^s(T_w-T_\infty)\,\mathrm{d}s\quad\text{and}\quad s=\int_0^\xi \mathrm{d}\xi \tag{25}$$

This gives

$$Nu_m\left(\frac{Gr}{5}\right)^{-1/5}=\frac{\int_0^\xi \mathrm{d}\xi}{\int_0^\xi \xi^{1/5}\theta(\xi,0)\,\mathrm{d}\xi} \tag{26}$$

III. Results and Discussion

Numerical results are presented for the non-Newtonian power-law fluids with shear-thinning ($n=0.6$ and 0.8) and shear-thickening ($n=1.2$ and 1.4) as well as for the Newtonian case ($n=1$). Two sets of the threshold values for shear rates defined in Eq. (4) $(\gamma_1,\gamma_2)\approx(0.1,10^5)$ and $(\gamma_1,\gamma_2)\approx(0.01,10^5)$ are used in the computations. An example of the modified power law appears in Fig. 1.

The computer code, similar to the one used in [18], has shown an excellent agreement with the results of Mahajan and Gebhart [20] for a Newtonian fluid, as demonstrated in Table 1. We believe that the accuracy of the code is preserved for non-Newtonian fluids. All results presented in the paper were checked by varying the grid sizes to warrant the convergence of numerical results.

Figures 3a and 3b show the viscosity distribution D as a function of η at selected ξ locations for $Pr=100$ and 1000, respectively, for the first set of threshold shear rates and $\xi=0.6$. From Fig. 3a, it is found for $Pr=100$ that there is only one region of variable viscosity at $\xi=60$, but there are two such regions at $\xi=80$, 100, 120, and 150; the primary region lies from $\eta\approx 0.0$ to 0.028, and the secondary variable-viscosity region lies between $\eta\approx 0.4875$ and 1.745. On the other hand, only one variable-viscosity region was found in the case of $Pr=1000$. For the second set of threshold shear rates, the viscosity distributions are presented in Figs. 4a and 4b. It is clearly

Table 1 Comparisons of the present numerical results with those of Mahajan and Gebhart [20] for $n=1.0$ (Newtonian fluid)

	$C_f[Gr/5\xi)^2]^{1/5}$		$\theta(\xi,0)$	
Pr	Mahajan and Gebhart [20]	Present results	Mahajan and Gebhart [20]	Present results
0.733	0.8089306	0.80892928	1.4798071	1.47980833
6.7	0.3563320	0.35633063	0.8417020	0.84170328

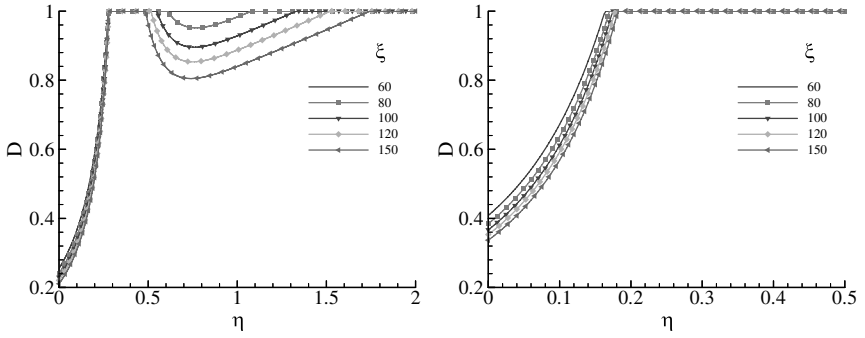

Fig. 3 Viscosity distribution at different ξ: a) $Pr = 100$ and b) $Pr = 1000$; $n = 0.6$, $\gamma_1 = 0.1$, and $\gamma_2 = 10^5$.

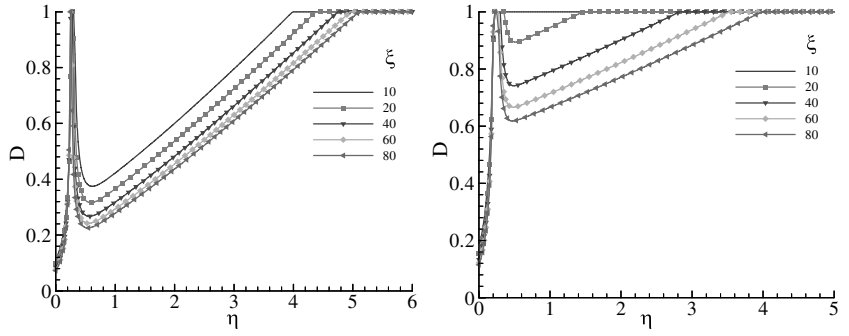

Fig. 4 Viscosity distribution at different ξ: a) $Pr = 100$ and b) $Pr = 1000$; $n = 0.6$, $\gamma_1 = 0.01$, and $\gamma_2 = 10^5$.

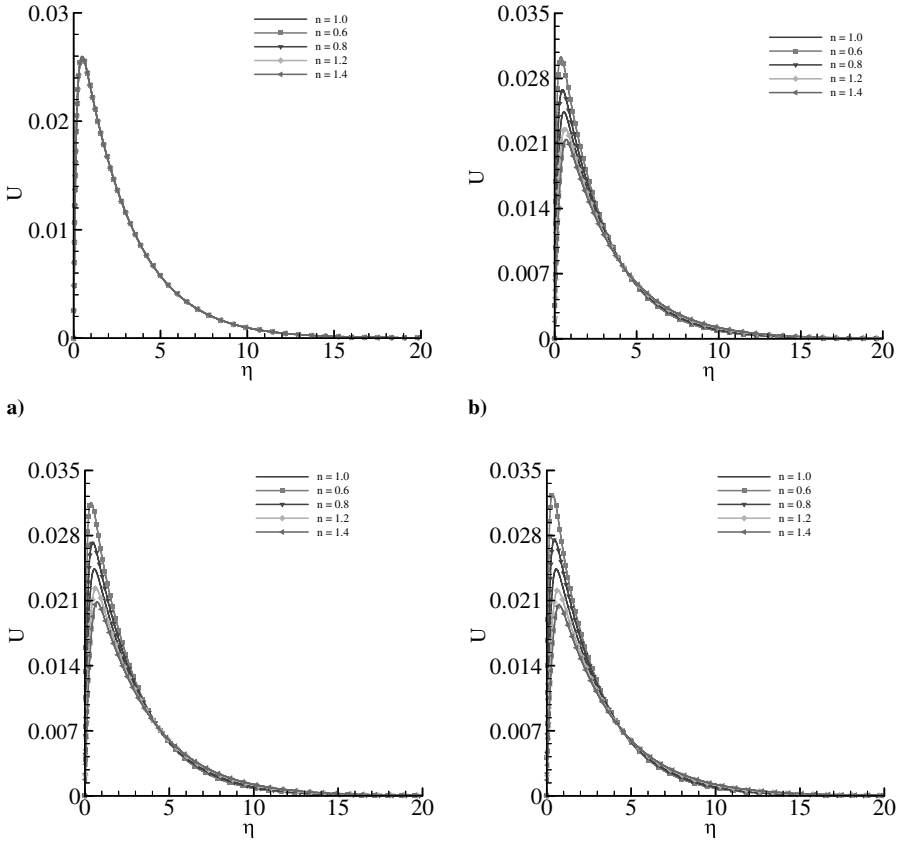

Fig. 5 Velocity distribution for the different n at a) $\xi = 0.0$, b) $\xi = 50.0$, c) $\xi = 100.0$, and d) $\xi = 150.0$; $Pr = 100$, $\gamma_1 = 0.1$, and $\gamma_2 = 10^5$.

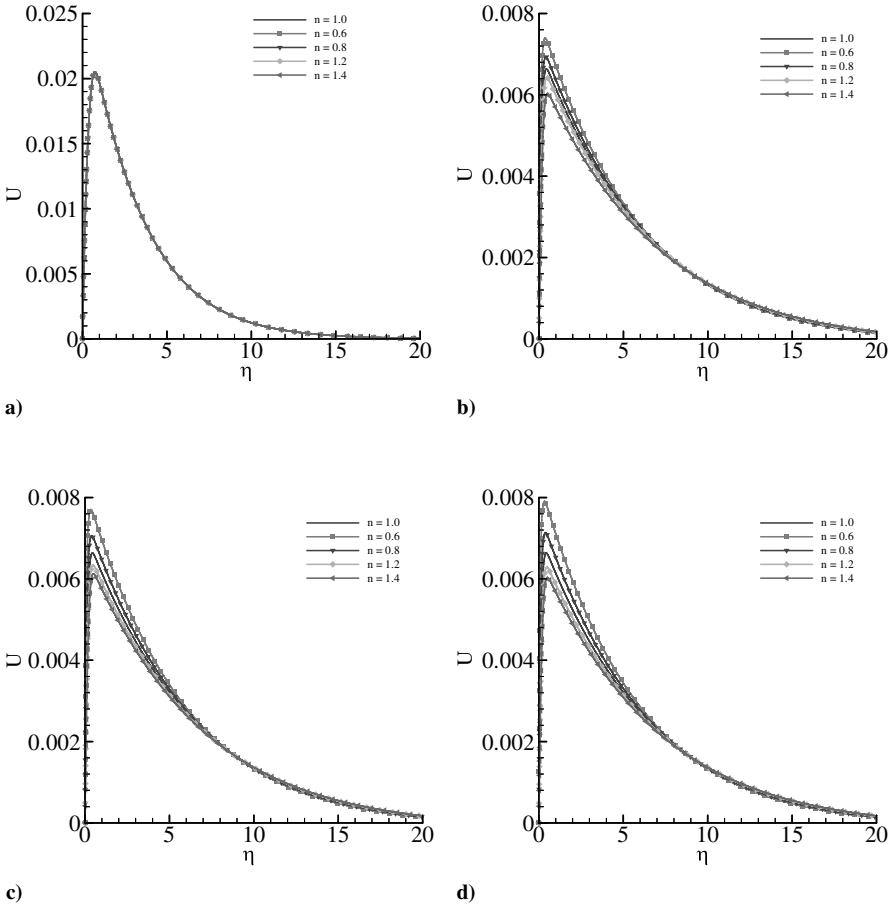

Fig. 6 Velocity distribution for the different n at a) $\xi = 0.0$, b) $\xi = 50.0$, c) $\xi = 100.0$, and d) $\xi = 150.0$; $Pr = 1000$, $\gamma_1 = 0.1$, and $\gamma_2 = 10^5$.

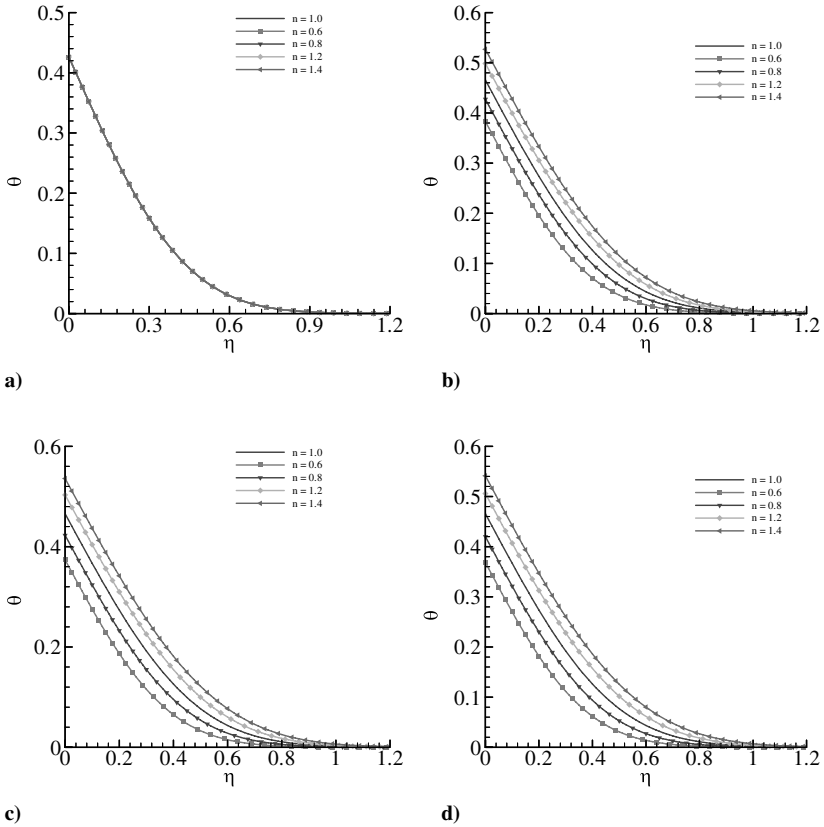

Fig. 7 Temperature distribution for the different n at a) $\xi = 0.0$, b) $\xi = 50.0$, c) $\xi = 100.0$, and d) $\xi = 150.0$; $Pr = 100$, $\gamma_1 = 0.1$, and $\gamma_2 = 10^5$.

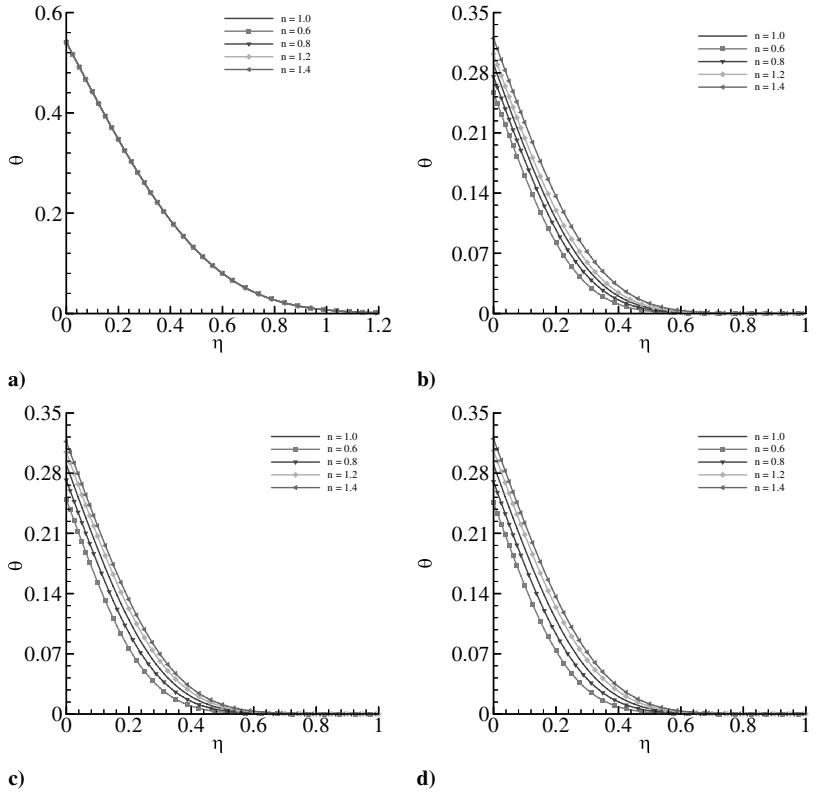

Fig. 8 Temperature distribution for the different n at a) $\xi = 0.0$, b) $\xi = 50.0$, c) $\xi = 100.0$, and d) $\xi = 150.0$; $Pr = 1000$, $\gamma_1 = 0.1$, and $\gamma_2 = 10^5$.

seen that the second region of the non-Newtonian viscosity develops within the boundary layer for both Prandtl numbers. From Fig. 4a, the secondary region of non-Newtonian viscosity appears from $\xi = 10$ in the case of $Pr = 100$, but from $\xi = 20$ for $Pr = 1000$. This is simply a consequence of the shear rate near the plate reaching the threshold value first; the region near the maximum axial velocity has a very small shear rate, and the shear rate grows slower in the region between the maximum axial velocity location and the edge of the boundary layer. Also, the natural-convection boundary layer takes a longer distance to develop for larger Prandtl numbers.

The velocity distribution as a function of η at the selected locations ($\xi = 0.0$, 50.0, 100.0, and 150.0) for the different power-law indices

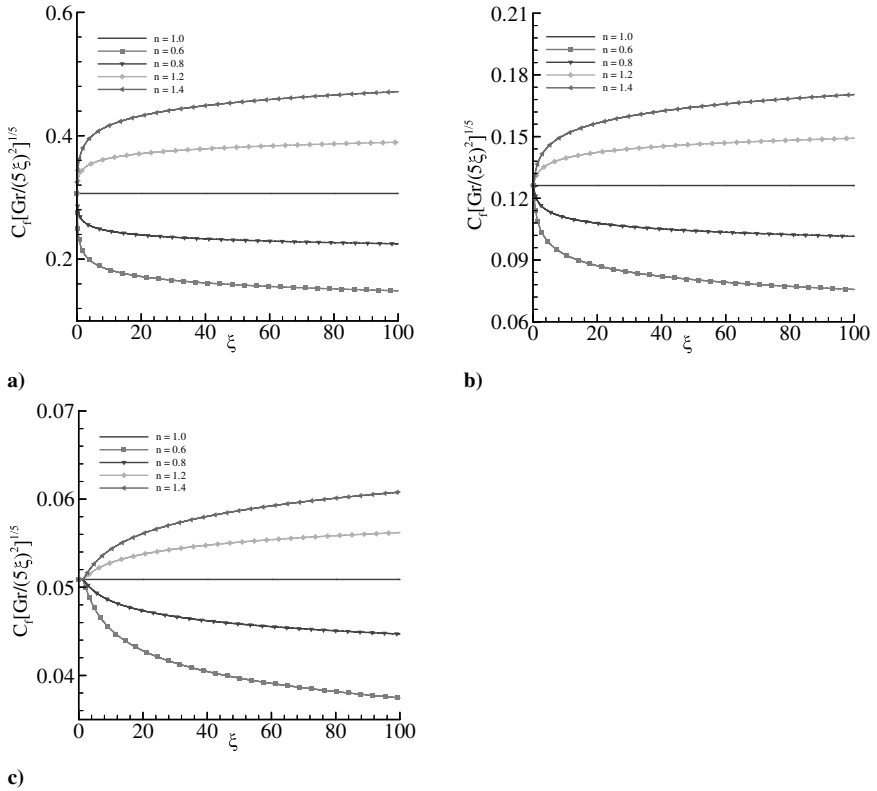

Fig. 9 Wall Shear stress for different values of n: a) $Pr = 10$, b) $Pr = 100$, and c) $Pr = 1000$; $\gamma_1 = 0.1$ and $\gamma_2 = 10^5$.

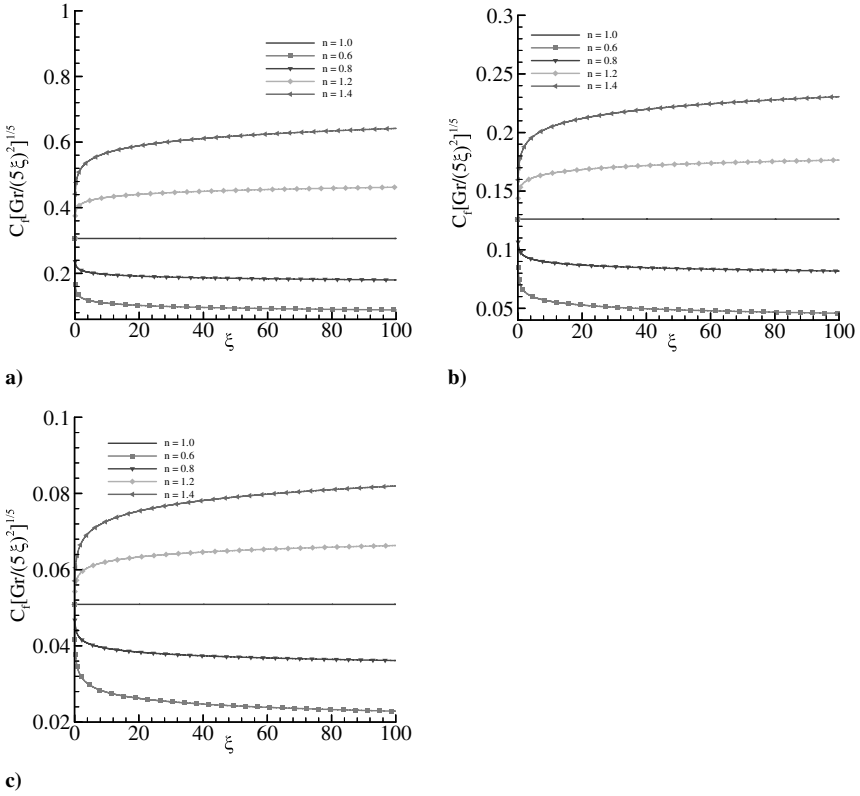

Fig. 10 Wall shear stress for the different values of n: a) $Pr = 10$, b) $Pr = 100$, and c) $Pr = 1000$; $\gamma_1 = 0.01$ and $\gamma_2 = 10^5$.

($n = 0.6$, 0.08, 1.0, 1.2, and 1.4) are presented in Figs. 5 and 6 for $Pr = 100$ and 1000, respectively. The threshold shear rates are $(\gamma_1, \gamma_2) = (0.1, 10^5)$. Because the value of D equals 1.0 at the leading edge, the distribution of the axial velocity is a similarity profile. Figures 5b–5d and 6b–6d show that for shear-thinning fluids ($n = 0.6$ and 0.8), the velocity increases due to the decrease of viscosities at the downstream region; consequently, the boundary layer is thinned. On the other hand, for shear-thickening fluids ($n = 1.2$ and 1.4), the velocity decreases slowly and the boundary layer is thickened as the fluid becomes more viscous. We can

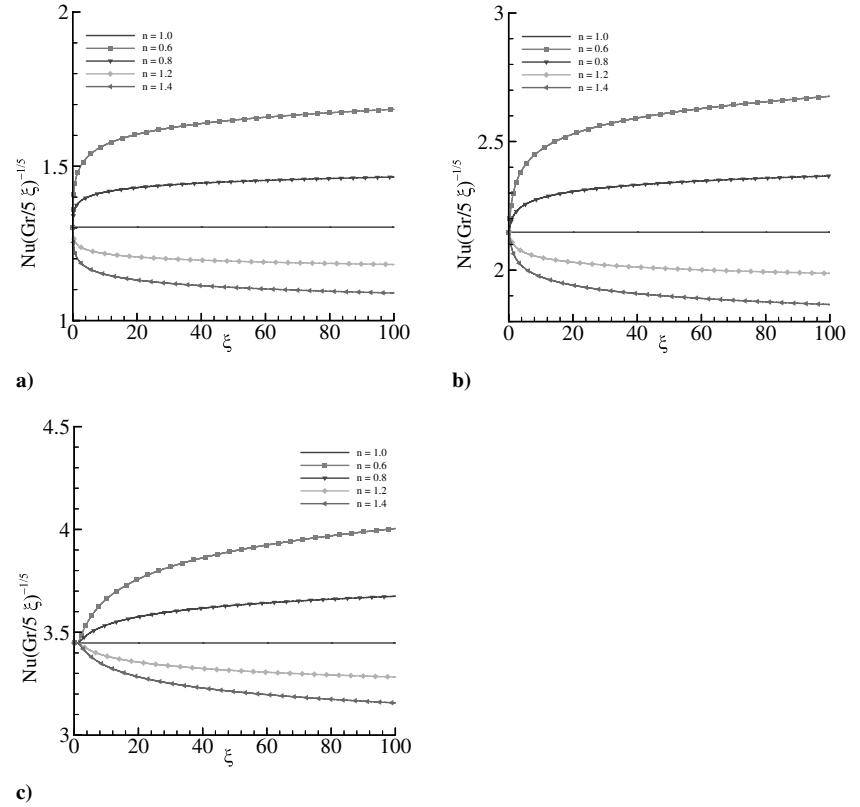

Fig. 11 Local Nusselt number for different values of n: $Pr = 10$, b) $Pr = 100$, and c) $Pr = 1000$; $\gamma_1 = 0.1$ and $\gamma_2 = 10^5$.

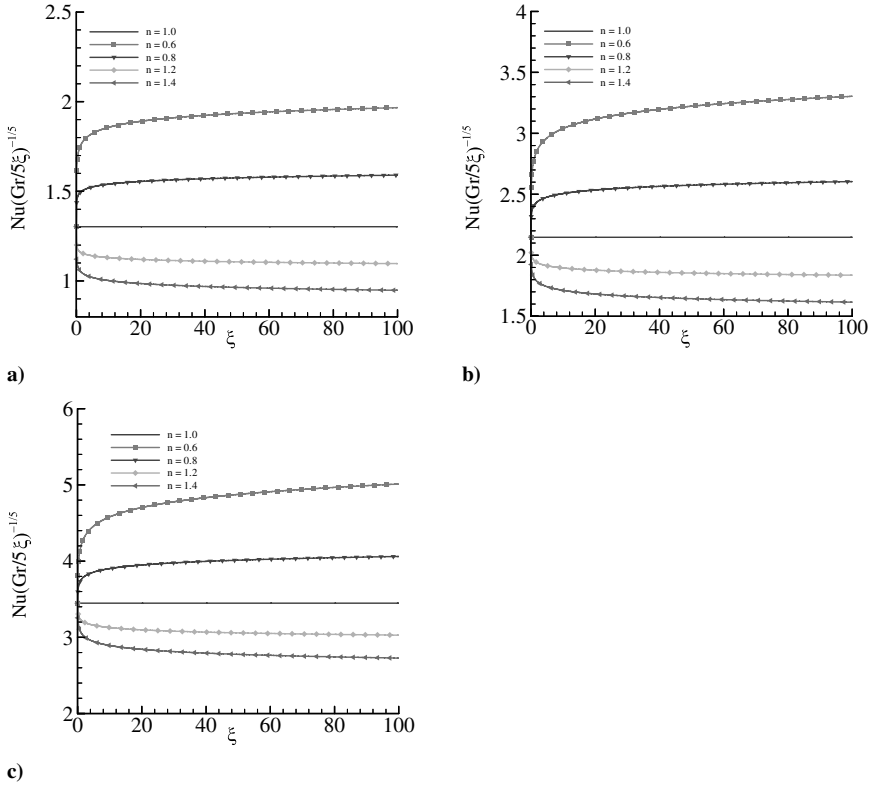

Fig. 12 Local Nusselt number for different values of n: a) $Pr = 10$, b) $Pr = 100$, and c) $Pr = 1000$; $\gamma_1 = 0.01$ and $\gamma_2 = 10^5$.

conclude that for $Pr = 1000$, the fluid velocity is smaller than the velocity for $Pr = 100$, and the boundary-layer thickness is greater for $Pr = 1000$ than for $Pr = 100$.

Figures 7 and 8 depict the corresponding temperature distributions for $Pr = 100$ and 1000, respectively. Similar to the velocity distribution at $\xi = 0.0$, the temperature distribution is a similarity solution at the leading edge. At the downstream region, in the case of shear-thinning fluids, the variation of temperature in the boundary layer is smaller than that of the shear-thickening non-Newtonian fluids. As expected, the thermal boundary layer is thinner for larger Prandtl numbers.

The effects of the non-Newtonian power-law index $n = 0.6$, 0.8, 1.0, 1.2, and 1.4 on the variation of the wall shear stress $C_f[Gr/(5\xi)^2]^{1/5}$ are illustrated with $(\gamma_1, \gamma_2) = (0.1, 10^5)$ in

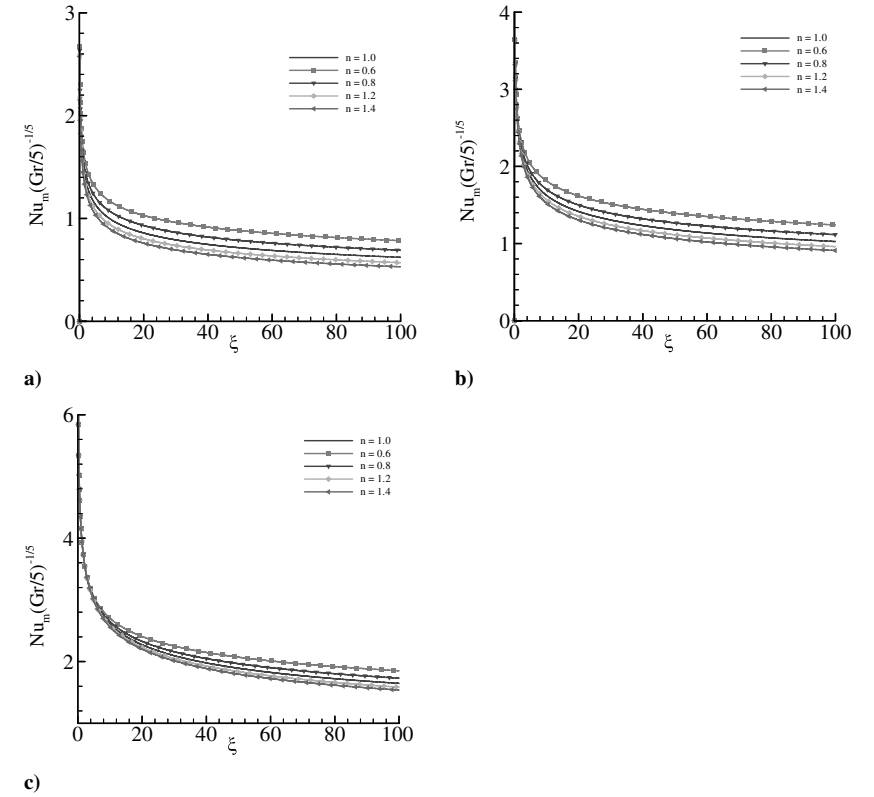

Fig. 13 Average Nusselt number for the different values of n: a) $Pr = 10$, b) $Pr = 100$, and c) $Pr = 1000$; $\gamma_1 = 0.1$ and $\gamma_2 = 10^5$.

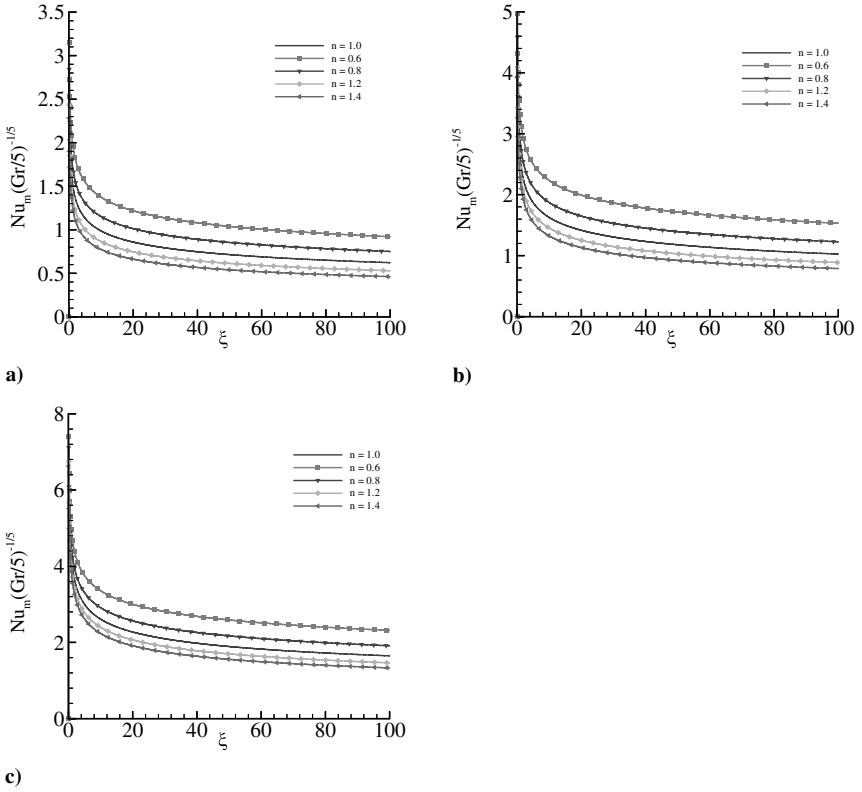

Fig. 14 Average Nusselt number for the different values of n: a) $Pr = 10$, b) $Pr = 100$, and c) $Pr = 1000$; $\gamma_1 = 0.01$ and $\gamma_2 = 10^5$.

Figs. 9a–9c for $Pr = 10$, 100, and 1000, respectively. The results from these figures clearly show that the wall shear stress decreases for the shear-thinning fluids ($n = 0.6$ and 0.8), and increases for shear-thickening fluids ($n = 1.2$ and 1.4). For the case $(\gamma_1, \gamma_2) = (0.1, 10^5)$, non-Newtonian effects start from $\xi > 0.01$ for $Pr = 10$ and $\xi > 0.2$ for $Pr = 100$, but this effect exists from $\xi > 1.0$ for $Pr = 1000$. It is important to notice that the similarity solution is valid before the non-Newtonian effects begin downstream from the leading edge. After the non-Newtonian effects turn up, the similarity solution becomes invalid further downstream. This clearly indicates that the length scale is introduced into the boundary-layer formulation by the classical power-law correlation; consequently, no self-similar solution is possible.

For the second case, $(\gamma_1, \gamma_2) = (0.01, 10^5)$, the wall shear stresses are shown in Figs. 10a–10c for $Pr = 10$, 100, and 1000, respectively. Because the triggering shear rate is much smaller, the effects of non-Newtonian fluids surface much earlier than for the first case.

The local rate of heat transfer in terms of the local Nusselt number $Nu(Gr/5\xi)^{-1/5}$ are plotted in Figs. 11 and 12 for $(\gamma_1, \gamma_2) = (0.1, 10^5)$ and $(0.01, 10^5)$, respectively. The local Nusselt number increases for $n > 1$ and decreases for $n < 1$. Thus, the rate of heat transfer is enhanced for the shear-thinning fluids and reduced for the shear-thickening fluids. The results are different for the two sets of threshold-shear-rate limits. It takes a longer distance for non-Newtonian effects to surface for $(\gamma_1, \gamma_2) = (0.1, 10^5)$ than for $(\gamma_1, \gamma_2) = (0.01, 10^5)$, as expected.

Figures 13 and 14 depict the average rate of heat transfer in terms of the average Nusselt number $Nu_m(Gr/5)^{-1/5}$ for $(\gamma_1, \gamma_2) = (0.1, 10^5)$ and $(0.01, 10^5)$, respectively. From these figures, it is clearly seen that the convective heat transfer decreases along the plate whether the fluid is Newtonian or non-Newtonian.

IV. Conclusions

The proposed modified power-law correlation agrees well with the actual measurements for non-Newtonian fluids; consequently, it is a physically realistic model. It is noteworthy that for the different values of the threshold shear rates, the obtained results are also different. Thus, it is important to make use of accurate measurements of the non-Newtonian flow quantities. For the shear-thinning fluids, the shear stress increases and the rate of heat transfer decreases, and for the shear-thickening fluids, the opposite results are observed.

References

[1] Hinch, J., "Non-Newtonian Geophysical Fluid Dynamics," Woods Hole Oceanographic Inst., Woods Hole, MA, 2003.

[2] Acrivos, A., "A Theoretical Analysis of Laminar Natural Convection Heat Transfer to Non-Newtonian Fluids," *AIChE Journal*, Vol. 6, No. 4, 1960, pp. 584–590. doi:10.1002/aic.690060416

[3] Tien, C., "Laminar Natural Convection Heat Transfer to Non-Newtonian Fluids," *Applied Scientific Research*, Vol. 17, 1967, pp. 233–248. doi:10.1007/BF00386093

[4] Emery, F. H., Chi, S., and Dale, J. D., "Free Convection Through Vertical Plane Layers of Non-Newtonian Power Law Fluids," *Journal of Heat Transfer*, Vol. 93, 1970, pp. 164–171.

[5] Dale, J. D., and Emery, A. F., "The Free Convection of Heat from a Vertical Plate to Several Non-Newtonian Pseudo Plastic Fluids," *Journal of Heat Transfer*, Vol. 94, 1972, pp. 64–72.

[6] Chen, T. V. W., and Wollersheim, D. E., "Free Convection at a Vertical Plate with Uniform Flux Conditions in Non-Newtonian Power Law Fluids," *Journal of Heat Transfer*, Vol. 95, 1973, pp. 123–124.

[7] Shulman, Z. P., Baikov, V. I., and Zaltsgendler, E. A., "An Approach to Prediction of Free Convection in Non-Newtonian Fluids," *International Journal of Heat and Mass Transfer*, Vol. 19, No. 9, 1976, pp. 1003–1007. doi:10.1016/0017-9310(76)90182-4

[8] Som, A., and Chen, J. L. S., "Free Convection of Non-Newtonian Fluids over Nonisothermal Two-Dimensional Bodies," *International Journal of Heat and Mass Transfer*, Vol. 27, No. 5, 1984, pp. 791–794. doi:10.1016/0017-9310(84)90148-0.

[9] Haq, S., Kleinstreuer, C., and Mulligan, J. C., "Transient Free Convection of a Non-Newtonian Fluid Along a Vertical Wall," *Journal of Heat Transfer*, Vol. 110, 1988, pp. 604–607.

[10] Huang, M. J., Huang, J. S., Chou, Y. L., and Cheng, C. K., "Effects of Prandtl Number on Free Convection Heat Transfer from a Vertical Plate to a Non-Newtonian Fluid," *Journal of Heat Transfer*, Vol. 111, Feb. 1989, pp. 189–191.

[11] Huang, M. J., and Chen, C. K., "Local Similarity Solutions of Free-Convective Heat Transfer From a Vertical Plate to Non-Newtonian

Power Law Fluids," *International Journal of Heat and Mass Transfer*, Vol. 33, No. 1, 1990, pp. 119–125. doi:10.1016/0017-9310(90)90146-L

[12] Kim, E., "Natural Convection Along a Wavy Vertical Plate to Non-Newtonian Fluids," *International Journal of Heat and Mass Transfer*, Vol. 40, No. 13, 1997, pp. 3069–3078. doi:10.1016/S0017-9310(96)00357-2

[13] Khan, W. A., Culham, J. R., and Yovanovich, M. M., "Fluid Flow and Heat Transfer in Power Law Fluids Across Circular Cylinders: Analytical Study," *Journal of Heat Transfer*, Vol. 128, Sept. 2006, pp. 870–878. doi:10.1115/1.2241747

[14] Denier, J. P., and Hewitt, R. E., "Asymptotic Matching Constraints for a Boundary-Layer Flow of a Power Law Fluid," *Journal of Fluid Mechanics*, Vol. 518, 2004, pp. 261–279. doi:10.1017/S0022112004001090

[15] Denier, J. P., and Dabrowski, P. P., "On the Boundary-Layer Equations for Power-Law Fluids," *Proceedings of the Royal Society of London, Series A: Mathematical and Physical Sciences*, Vol. 460, No. 2051, 2004, pp. 3143-3158. doi:10.1098/rspa.2004.1349

[16] Yao, L. S., and Molla, M. M., "Flow of a Non-Newtonian Fluids on a Flat Plate, 1: Boundary Layer," *Journal of Thermophysics and Heat Transfer* (to be published).

[17] Molla, M. M., and Yao, L. S., "Flow of a Non-Newtonian Fluids on a Flat Plate, 2: Heat Transfer," *Journal of Thermophysics and Heat Transfer* (to be published).

[18] Molla, M. M., Hossain, M. A., and Yao, L. S., "Natural Convection Along a Vertical Complex Wavy Surface with Uniform Heat Flux," *Journal of Heat Transfer*, Vol. 129, Oct. 2007, pp. 1403–1407. doi:10.1115/1.2755062

[19] Yao, L. S., and Molla, M. M., "Forced Convection of Non-Newtonian Fluids on a Heated Flat Plate," *International Journal of Heat and Mass Transfer* (to be published).

[20] Mahajan, R. L., and Gebhart, B., "Higher Order Approximation to the Natural Convection Flow over a Uniform Flux Vertical Surface," *International Journal of Heat and Mass Transfer*, Vol. 21, No. 5, 1978, pp. 549–556. doi:10.1016/0017-9310(78)90051-0